Chalcogenide Letters Vol. 21, No. 10, October 2024, p. 765 - 770

Photocatalytic and thermoelectric properties of Cu_2SrSnS_4 nanoparticles by solvothermal method

G. Hao*, J. Y. Shen, Y. L. Sun, K. Xu, Y. F. Wang
School of Materials Science and Engineering, Yancheng Institute of Technology, 9 Yinbing Street, Yancheng 224051, PR China

In the present work, flower-like Cu_2SrSnS_4 (CSTS) sample is successfully prepared by solvothermal method. The XRD and Raman analysis confirm that pure CSTS phase with trigonal structure is obtained. The band gap of as-obtained CSTS naocrystals is estimated to be 1.49eV. The removal of methylene blue (MB) within 100min under simulated solar light irradiation is around 90%, depicting that CSTS is a potential material for effective solar light photocatalytic application. Meanwhile, The Seebeck coefficient and electrical conductivity of CSTS material can reach to 128.57μV•K^{-1} and 20.35S·m^{-1} at 675K, respectively, indicating its potential for thermoelectric application.

(Received July 1, 2024; Accepted October 2, 2024)

Keywords: Semiconductor, Cu_2SrSnS_4, Nanocrystals, Solvothermal, Photocatalytic, Electrical transport

1. Introduction

In the course of industrialization for recent decades, water pollution and energy crisis are becoming two overwhelming problems over the world. Many researchers have focused on environmentally-friendly and energy conversion materials. A novel quaternary chalcogenide compound, Cu_2ZnSnS_4(CZTS) occupies a special place in many fields such as photovoltaic, photocatalytic and thermoelectric applications owing to its optimum optical band energy of about 1.5eV, absorption coefficient of higher than 10^4 cm^{-1} and low lattice thermal conductivity [1-6]. However, CZTS is facing a problem of anti-site defects caused by the similarity in the ionic radius of Cu^+ and Zn^{2+}, which result in carrier recombination. A novel solution of prevent anti-defects is studied by replacing Zn^{2+} with larger sized Sr^{2+}. Meanwhile, Cu_2SrSnS_4 known as CSTS can retain the structure and property similar to CZTS, which is also recognized as an excellent alternative material for energy application [7-8]. Over the past few years, Only a few reports have been found to study CSTS compounds using theoretical and experimental research, which are mainly focused on in the field of solar cell devices [9-16].

In this research work, the present study reports a facile solvothermal method to prepare CSTS nanoparticles. The structure, morphology, photocatalytic and electrical transport performances of CSTS nanoparticles are systematically investigated.

2. Experimental details

All chemical reagents, including Cupric nitrate ($Cu(NO_3)_2·3H_2O$), Strontium acetate ($Sr(CH_3COO)_2·0.5H_2O$), Tin dichloride ($SnCl_2·2H_2O$) and Thiocarbamide (H_2NCSNH_2), are received from Sinophram chemical reagent Corporation, and all materials are used further without

* Corresponding author: guanhao1980@sina.com
https://doi.org/10.15251/CL.2024.2110.765

purification. In the synthetic procedure, the precursor is prepared by dissolving 2mMol Cupric nitrate, 1mMol Strontium acetate, 1mMol Tin dichloride and 6mMol Thiocarbamide in 80ml ethylene glycol (EG) as the solvent agent. The homogeneous solution is prepared after continue stirring for 3h, then the solution is solvothermally treated in autoclave of 100ml capacity at 200℃ for 24h. At last, the obtained products are isolated by adding distilled water and purified by centrifugation repeatedly after cooling down to room temperature naturally, and dried at 80℃ under vacuum for 3h, which are collected and further used. In a thermoelectric experiment, CSTS nanoparticles are utilized to prepare pellet sample by applying 60MPa pressure and sintering 500℃ for 1h under vacuum condition.

The structure of synthesized CSTS is analyzed using PaNalytical X'Pert Pro diffractometer and JY-T64000 Raman spectrometer. The surface morphological analysis is done using LEO-1530VP scanning electron microscopy. The optical and photocatalytic studies are performed by using Varian Cary 5000 spectrophotometer and Shimadzu UV2450 spectrophotometer. The electrical transport performances are carried out using Namicro-III thermoelectric system in temperature range from 325K to 675K.

3. Results and discussion

The structural analysis measurements are depicted in Fig.1. It is observed from Fig.1(a) that obviously seven characteristic peaks of CSTS (PDF NO.30-0504) at 2θ angles equal to 24.1°, 28.5°, 32.6°, 37.1°, 40.6°, 47.2° and 55.6° corresponding to (103), (110), (105), (203), (204), (213) and (118) planes are clearly noted, indicating a single-phase CSTS is obtained. The nanocrystalline in nature can be evaluated from the broad Full Width Half Maximum (FWHM). Furthermore, the average crystallite size is calculated to be about 25.8nm using Debye-Scherrer formula. Raman spectroscopy is further implied to confirm the XRD analysis because of the similarity of the XRD patterns of some phases. Raman spectrum of CSTS nanocrystals is depicted in Fig.1(b). It is found that only the main peak located at 343cm^{-1} is observed, which is correspond to the trigonal structure of CSTS sample. The possible impurity phases such as $Cu_{2-x}S$ (275, 315 and 475cm^{-1}) and Cu_2SnS_3 (290, 318 and 348 cm^{-1}) are excluded.

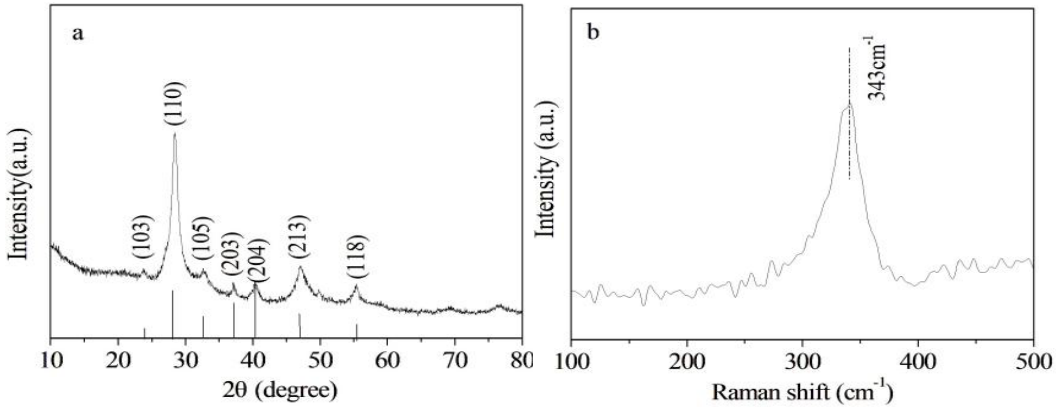

Fig. 1. XRD pattern(a) and Raman spectrum(b) of CSTS nanoparticles.

Fig. 2 shows the morphology of pristine CSTS sample. We can observe that CSTS nanoparticles are composed of flower-like morphology by self-assembling of nano sheet-like structures. The growth mechanism such as nucleation, nanosheet growth orientation and self-assemble action is in agreement with experimental results in literature [17-18]. High magnification image shows the average thickness of each nanosheet is about 25nm, while low

magnification image exhibits uniform distribution. The flower-shape particles with large surface area can enhance more absorption sites, lead to improvement of catalytic efficiency [19]. Meanwhile, the nanosheet structure with a large number of grain boundaries can enhance phonon scattering, result in decreasing the thermal conductivity [20].

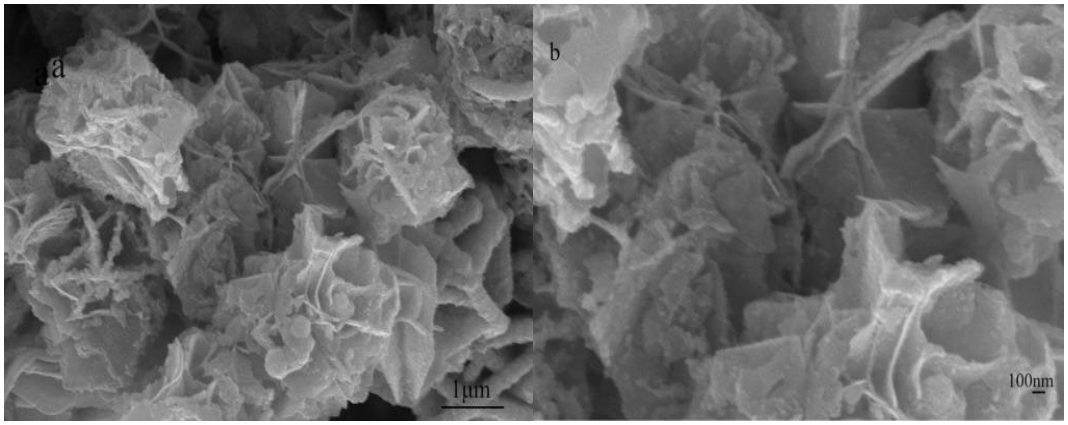

Fig. 2. Low magnification(a) and high magnification(b) SEM images of CSTS nanoparticles.

The UV-Vis absorption spectrum is displayed in Fig.3. We can observe that CSTS sample exhibits strong and broad absorption band over entire visible region and its tail extends to IR region. As shown in the set, the band gap of CSTS nanocrystals is calculated to be 1.49eV using Tauc formula by plotting the linear region of $(\alpha h\nu)^2$ vs. $h\nu$, which is proper band gap energy required for catalytic semiconductor material. The value is low compared to those reported by several researchers [10, 13-14], it may be attributed to quantum confinement effect and the formation of microstrain owing to increasing grain sizes.

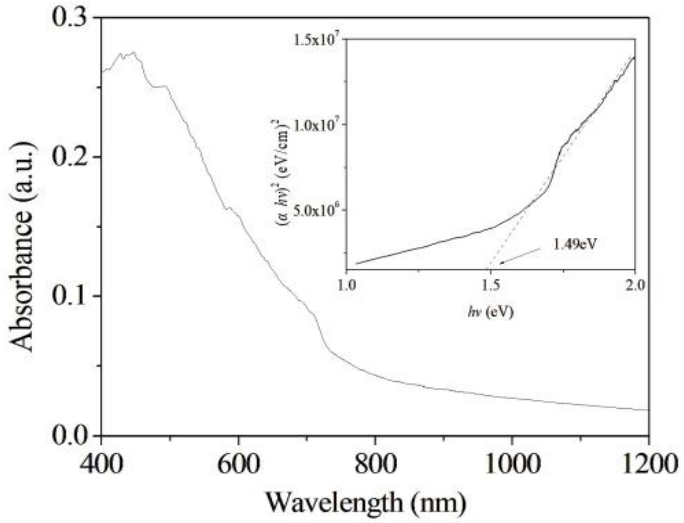

Fig. 3. UV-Vis spectrum of CSTS nanoparticles; Inset: Optical bandgap estimation of CSTS nanoparticles.

The photocatalysis activity of CSTS nanoparticles is examined by degradation of methylene blue (MB) under simulated solar light irradiation in 100min. The efficiencies of degradation against the time of light exposure are presented in Fig.4(a). We can observe that about 2% of MB is removed without CSTS nanoparticles while that with the addition of CSTS shows the removal rate falls to 90% after 100min illumination, indicating that CSTS plays an important role on the degradation of MB. This result suggests that CSTS material opens up a door to visible-light photocatalytic application. The cycling performance of CSTS nanocrystals for the degradation of MB are studied. As depicted in Fig.4(b), the degradation rate only decreases from 90% to 88% after reuse three times, indicating reuse stability of CSTS photocatalyst. Furthermore, Fig.4(c) shows that the XRD patterns of CSTS nanocrystals after use has no obviously change compare to those before use, confirming the structural stability.

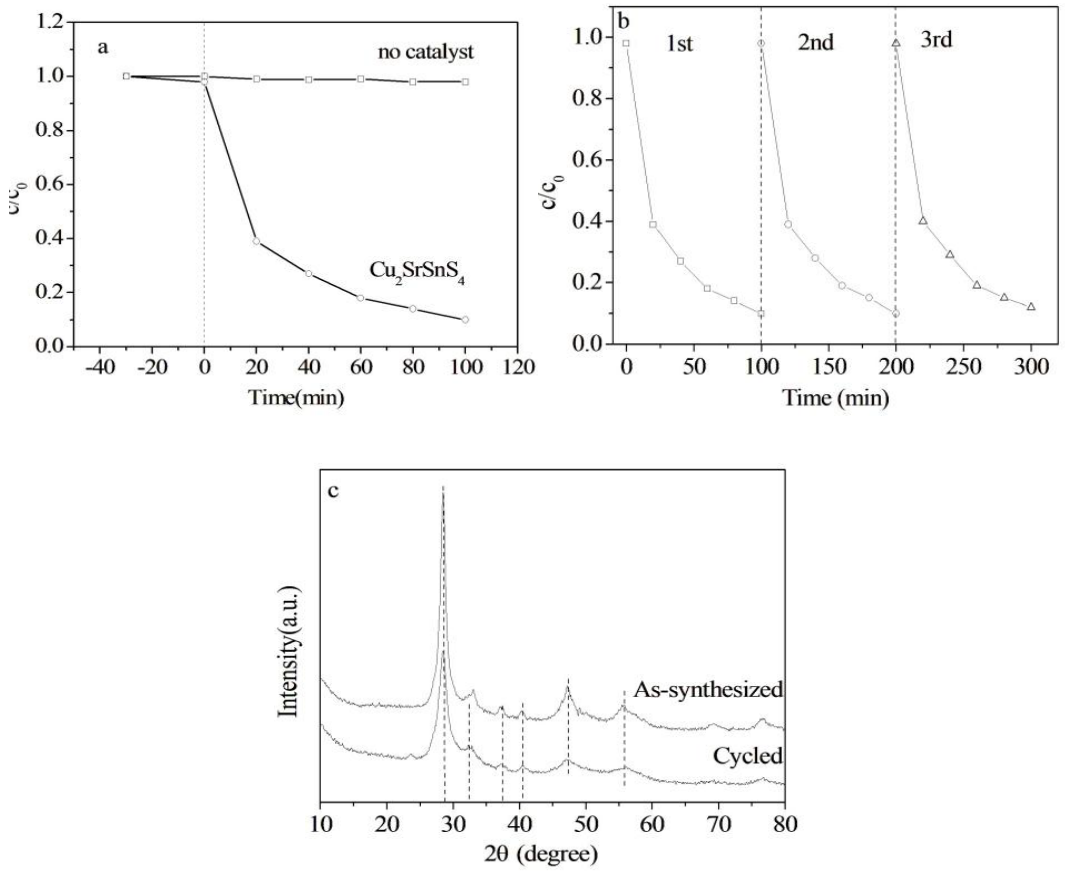

Fig.4 (a)the efficiencies of degradation of MB as a function of different time (b) the photo stability of CSTS nanoparticles (c) the structural stability of CSTS nanoparticles.

The variation in Seebeck coefficient (S) and electrical conductivity (σ) of CSTS sample as a function of temperature are plotted in Fig.5. It is observed that CSTS sample exhibits *P*-type semiconductor behavior owing to the positive Seebeck coefficient values. The Seebeck coefficient and electrical conductivity of CSTS sample increase with increasing measured temperature. CSTS

nanocrystals show a high Seebeck coefficient value of 128.57μV•K^{-1} while the value of electrical conductivity reaches to 20.35S·m^{-1} at 675K.

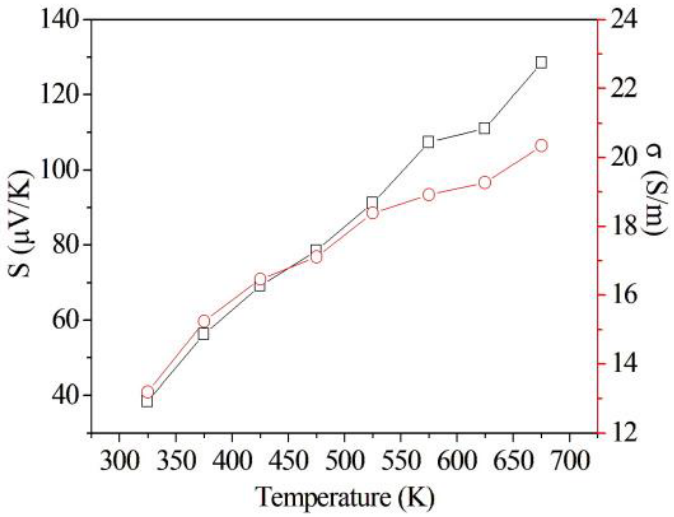

Fig. 5. Temperature-dependent plot of Seebeck coefficient and electrical conductivity of CSTS sample.

4. Conclusions

In the work, *P*-type semiconductor material Cu_2SrSnS_4(CSTS) with trigonal structure is synthesized via solvothermal approach. The flower-like morphology being composed of nano sheet-like is confirmed. Cu_2SrSnS_4 nanocrystals with the narrow band gap of 1.49eV remove 90% of the methylene blue (MB) in 100min under simulated solar light irradiation, depicting a promise in treatment of water pollutants. The large Seebeck coefficient and moderate electrical conductivity of Cu_2SrSnS_4 sample are obtained, which indicates that Cu_2SrSnS_4 is a promising material for thermoelectric application.

References

[1] Z. Zhou, Y. Wang, D. Xu, Y. Zhang, Sol. Energy Mater. Sol. Cells 94, 2042 (2010); https://doi.org/10.1016/j.solmat.2010.06.010

[2] J. Huang, C. Yan, K. Sun, F. Liu, H. Sun, A. Pu, X. Liu, M. Green, X. Hao, Sol. Energy Mater. Sol. Cells 175, 71 (2018); https://doi.org/10.1016/j.solmat.2017.10.009

[3] R. Henríquez, P. S. Nogales, P. G. Moreno, E. M. Cartagena, P. L. Bongiorno, E. Navarrete-Astorga, E. A. Dalchiele, Nanomaterial 1731, 13(2023); https://doi.org/10.3390/nano13111731

[4] S. Manjula, A. Sarathkumar, G. Sivakumar, Journal of Nano Research 79, 25 (2023); https://doi.org/10.4028/p-b6b546

[5] K. Gupta, S. Gupta, Y. Batra, Mat. Sci. Eng. B-Adv. 303, 117291 (2024); https://doi.org/10.1016/j.mseb.2024.117291

[6] B. D. Long, L. H. Thang, N. H. Hai, K. Suekuni, K. Hashikuni, T. Q. M. Nhat, W. Klich, M. Ohtaki, Mat. Sci. Eng. B-Adv. 272, 115353 (2021); https://doi.org/10.1016/j.mseb.2021.115353

[7] R. Chakraborty, P. Ghosh, Appl. Surf. Sci. 570, 151049 (2021); https://doi.org/10.1016/j.apsusc.2021.151049

[8] F. Hong, W. Lin, W. Meng, Y. Yan, Phys. Chem. Chem. Phys. 18, 4828(2016); https://doi.org/10.1039/C5CP06977G

[9] Z. F. Tong, J. Y. Yuan, J. R. Chen, A. Q. Wu, W. W. Huang, C. C. Han, Q. J. Caia, C. H. Ma, Y. Liu, L. Fang, Z. F. Liu, Mater. Lett. 237, 130(2019); https://doi.org/10.1016/j.matlet.2018.11.083

[10] M. V. Gapanovich, E. V. Rabenok, F. K. Chikin, B. I. Golovanov, I. N. Odin, V. V. Rakitin, D. M. Sedlovets, D. V. Korchagin, G. V. Shilov, Mendeleev Commun. 33, 264(2023); https://doi.org/10.1016/j.mencom.2023.02.037

[11] A. K. Yadav, S. Ramawat, S. Kukreti, A. Dixit, Appl. Phys. A-Mater. 130, 28(2024); https://doi.org/10.1007/s00339-023-07184-x

[12] N. Y. Dzade, Sci. Rep. 11, 4755(2021); https://doi.org/10.1038/s41598-021-84037-8

[13] A. Crovetto, Z. D. Xing, M. Fischer, R. Nielsen, C. N. Savory, T. Rindzevicius, N. Stenger, D. O. Scanlon, I. Chorkendorff, P. C. K. Vesborg, ACS Appl. Mater. Interfaces 12, 50446(2021); https://doi.org/10.1021/acsami.0c14578

[14] H. R. Xiao, Z. Chen, K. W. Sun, C. Yan, J. Xiao, L. X. Jiang, X. J. Hao, Y. Q. Lai, F. Y. Liu, Thin Solid Films 697, 137828(2020); https://doi.org/10.1016/j.tsf.2020.137828

[15] Y. H. Chan, B. Kilic, M. M. Hirschmann, C. K. Chiu, L. M. Schoop, D. G. Joshi, A. P. Schnyder, Phys. Rev. Mater. 3, 124204(2019); https://doi.org/10.1103/PhysRevMaterials.3.124204

[16] T. Kokab, Z. Siddique, S. Hussain, A. Iqbal, J. Mater. Sci-Mater. El. 30, 20860(2019); https://doi.org/10.1007/s10854-019-02453-z

[17] T. X. Wang, Y. G. Li, H. R. Liu, H. Li, S. X. Chen, Mater. Lett. 124, 148(2014); https://doi.org/10.1016/j.matlet.2014.03.044

[18] H. Guan, H. J. Hou, M. N. Li, J. M. Cui, Mater. Lett. 188, 319(2017); https://doi.org/10.1016/j.matlet.2016.09.018

[19] A. Abbas, K. Li, X. Guo, A. Wu, F. Ali, S. Attique, A. Ahmad, Environ. Res. 205, 112539(2022); https://doi.org/10.1016/j.envres.2021.112539

[20] J. Mani, S. Radha, A.S. Alagar Nedunchezhian, R. Rajkumar, C.K. Amaljith, M. Arivanandhan, R. Jayavel, G. Anbalagan, J. Solid State Chem. 310, 123088(2022); https://doi.org/10.1016/j.jssc.2022.123088